
Article:
Noofeli, A., Hall, P. and Rennie, A.J.R. (2014) Ionic liquid based EDLCs: influence of carbon porosity on electrochemical performance. Faraday Discussions, 172. pp. 163-177. ISSN 1359-6640

https://doi.org/10.1039/C4FD00057A

Ionic Liquid based EDLCs: influence of carbon porosity on electrochemical performance

Asa Noofeli,[a] Peter J. Hall,[a] and Anthony J. R. Rennie[a]*

DOI: 10.1039/b000000x

Electrochemical double layer capacitors (EDLCs) are a category of supercapacitors, devices that store charge at the interface between electrodes and an electrolyte. Currently available commercial devices have a limited operating potential that restricts their energy and power densities. Ionic liquids (ILs) are a promising alternative electrolyte as they generally exhibit greater electrochemical stabilities and lower volatility. This work investigates the electrochemical performance of EDLCs using ILs that combine the bis(trifluoromethanesulfonyl) imide anion with sulfonium and ammonium based cations. Different activated carbon materials were employed to also investigate the influence of varying pore size on electrochemical performance. Electrochemical impedance spectroscopy (EIS) and constant current cycling at different rates were used to assess resistance and specific capacitance. In general, greater specific capacitances and lower resistances were found with the sulfonium based ILs studied, and this was attributed to their smaller cation volume. Comparing electrochemical stabilities indicated that significantly higher operating potentials are possible with the ammonium based ILs. The marginally smaller sulfonium cation performed better with the carbon exhibiting the largest pore width, whereas peak performance of the larger sulfonium cation was associated with a narrower pore size. Considerable differences between the performance of the ammonium based ILs were observed and attributed to differences not only in cation size but also due to the inclusion of a methoxyethyl group. The improved performance of the ether bond containing IL was ascribed to electron donation from the oxygen atom influencing the charge density of the cation and facilitating cation-cation interactions.

1 Introduction

Electrochemical Double Layer Capacitors (EDLCs) are a category of supercapacitors; electrical energy storage devices that have the ability to operate at substantially higher rates than similar sized electrochemical cells.[1] They typically exhibit long cycle lives (>500,000 cycles), display relatively high energy efficiencies and a high degree of reliability.[1-7] For these reasons, among others, they have become the subject of much research and are the theme of growing number of reviews.[2-12] To date, EDLCs have mainly been employed in applications where their useful traits allow for the design of systems that require less servicing/replacement than those based on batteries.[4-7, 9]

EDLCs store energy through the physical separation of charges at the interface between electrodes and an electrolyte, and are particularly useful when dealing with systems where variations in power demand leads to a large mismatch between the average and maximum power required. They are typically charged/discharged within

seconds and can display values of specific power up to 10kWkg^{-1}.[6, 7, 10]

An application where this is useful is in electric vehicles where there are rapidly changing demand profiles results in batteries being discharged at rates that cause reduced operating lifetimes.[4, 6] Employing EDLCs to cater for peak demand, alongside batteries or fuel cells, not only allows for the design of smaller, lighter systems but can increase the lifetime of the system and enables the efficient storage of high charging currents generated by regenerative braking systems.[13-15]

However EDLCs would be a more viable option for many applications if greater specific energy/energy densities could be achieved; this in turn is restricted by the operating voltage of the device. Operating voltage is defined by the electrochemical stability of the electrolyte, which limits not only the amount of energy that can be stored, but also the maximum rate at which energy can be delivered.

Equation 1 shows that the energy stored by an EDLC (E) varies with the capacitance (C) of the device, and with the square of the operating voltage (V):[1]

$$E = \frac{1}{2}CV^2$$

The maximum power (P), that can be delivered by an EDLC also varies quadratically with the the operating voltage and inversely with the equivalent series resistance (ESR) of the device, as shown in Equation 2:[1]

$$P = \frac{V^2}{ESR}$$

Equation 1 also shows that the majority of the useful energy (as well as higher quality energy[16]) is delivered at elevated potentials, and by considering the relationships in Equations 1 and 2, it is evident that increases in operating potential enhances both the energy and power delivered by EDLCs.

Commercially available devices are limited by decomposition of the electrolyte, which is typically acetonitrile or propylene carbonate based.[3, 5, 10, 12, 17] Ionic liquids (ILs) can possess relatively wide electrochemical stability windows (ESWs) allowing for significantly increased operating potentials. ILs are salts usually consisting of poorly interacting anions and cations; due to these weak interactions they display relatively low melting temperatures (<100ºC).[17-21] In addition, ILs typically possess several other physical properties that are desirable in EDLC electrolytes, such as non-flammability, high thermal and chemical stability, and due to their inherent low volatility can be considered to be less hazardous than organic solvent based electrolytes.[17, 22] Physical properties other than the ESW of ILs play a crucial role in their performance as electrolytes and vary considerably with the structure of their constituent ions. In particular, viscosity (which in turn influences conductivity) affects not only the capacitance of a device but the maximum power output.[23] High conductivities lead to a lower cell resistance, which remains a challenge in the case of ILs as their conductivity tends to be at least an order of magnitude lower than that of conventional electrolytes.

In this study we investigate the effect that cation structure has on the performance of IL based EDLCs using various cations paired with the bis(trifluoromethanesulfonyl) imide ([Tf_2N]) anion. The partially delocalized charge in the [Tf_2N] anion imparts some flexibility into the structure and results in weak interactions with cations.[24] This generally results in ILs with relatively low viscosities, wide ESWs and it has been shown that ILs containing this anion can

form a stable protective layer passivating the surface of aluminium current collectors.[25]

The most widely studied cations are pyrrolidinum or imidazolium based[17]. When coupled with the [Tf_2N] anion, pyrrolidinium based electrolytes are typically stable in the region of 3.5V; however, their relatively high viscosity results in poor performance at high rates.[17, 23, 26-28] Imidazolium [Tf_2N] electrolytes, on the other hand, tend to be less viscous at room temperature but are less electrochemically stable and are limited to operating potentials around 3.2V.[17, 20, 23, 29, 30] For example, the conductivity of 1-butyl-3-methylpyrrolidinum [Tf_2N] is in the region of 2.2mScm^{-1} [24] whereas 1-ethyl-3-methylimidazoium [Tf_2N] is 3.4mScm^{-1}.[29] There is therefore a compromise between the quantity of energy stored in an IL based EDLC and the rate at which this energy can be delivered.

In this work we report on the performance of ILs consisting of sulfonium and ammonium based cations coupled with the [Tf_2N] anion as EDLC electrolytes. Triethyl sulfonium [Tf_2N] exhibits a remarkably high conductivity of 7.1mScm^{-1} [31] and has been shown to exhibit relatively high values of specific capacitance when compared with a carbonate based electrolyte.[32] In the sulfonium based ILs used in this work the cation volume is smaller than that of the anion. To investigate the influence of carbon pore size on performance, bulkier ammonium cation based ILs were employed for comparative purposes.

The physical properties of ILs, in particular the viscosity/conductivity, can be altered through the inclusion of ether linkages in the alkyl side chains of cations.[33] It has been proposed that the inclusion of ether bonds results in increased specific capacitances in EDLCs using mesoporous carbon electrodes by adding a degree of flexibility into the anion and alteration of the charge density.[34] Therefore to explore this behaviour we compare the performance of butyl triethyl ammonium [N_{2224}] [Tf_2N] with that of N,N-diethyl-N-methyl-N(2-methoxyethyl) ammonium [$N_{221(1O2)}$] [Tf_2N].

As a substantial number of reports have shown that the pore characteristics of electrodes strongly influence the performance of EDLCs,[22, 28, 35-38] we also compare the behaviour of these ILs when combined with electrodes of differing average pore size (d) in the small mesopore range (i.e. 2<d<10nm).

2 Experimental

2.1 Carbon materials

Porous carbon materials were produced by carbonisation and physical activation of resorcinol-formaldehyde xerogels in a manner similar to that used in previous investigations.[23, 38, 39] The polycondensation of an aqueous solution of resorcinol, R (Aldrich, 99%) with formaldehyde, F (Aldrich, 37wt.%, stabilised with 10-15wt.% methanol) was catalysed by the addition of sodium carbonate, C (Aldrich, Na_2CO_3, >99.5%). R/F molar ratio was kept at 0.5 and R/W was 0.10gcm^{-3}. R/C ratios of 200, 250, 300 and 350 were used to control the pore characteristics of the resultant gels. Gelation occurred over the following 3 days at a temperature of 85ºC. Organic hydrogels then underwent solvent exchange with acetone before being dried at 80°C under vacuum.

Xerogels were carbonised in a tube furnace under flowing argon with a final temperature of 850°C being maintained for 180 mins. Physical activation under flowing CO_2 was then carried out in a tube furnace at a temperature of 850°C for 60 mins. The

activated carbon materials were ball milled under argon for 60 mins and stored under vacuum at 80ºC prior to use in electrodes/characterisation.

Nitrogen adsorption/desorption isotherms at -196ºC were obtained using a Micromeritics TriStar II 3020 instrument; samples were degassed at 200°C for 10h before analysis. Porosity distribution was evaluated using the original DFT model for nitrogen on carbon with slit shaped pores.

Electrodes were manufactured by mixing the carbon material with polymer binder (KynarFlex® 2801) in an 85/15 ratio by mass. An homogeneous slurry of this mixture with acetone was spread to a wet film thickness of 250 µm on 15 µm thick aluminium foil using a micrometer adjustable gap paint applicator. These sheets were dried under vacuum, cut into individual electrodes, and paired with those of identical mass to produce symmetrical cells.

2.2 Ionic liquids

The ionic liquids used in this study were purchased from Io-Li-Tec GmbH (Germany) and had a stated purity >99%. Figure 1 illustrates the structure of the ions contained in these ILs along with the abbreviated name used throughout this report.

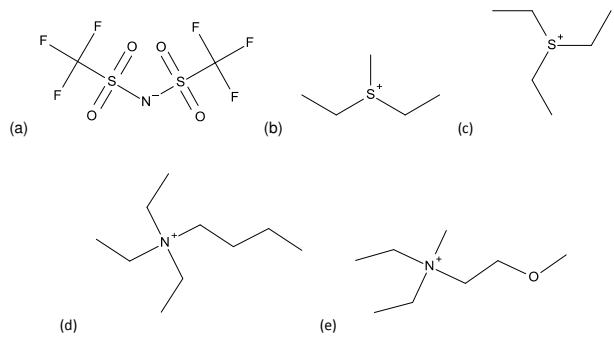

Fig. 1 Schematic structure of the constituent ions in the ionic liquids under study, (a) bis(trifluoromethanesulfonyl) imide [Tf_2N], (b) diethyl methyl sulfonium [S_{221}], (c) triethyl sulfonium [S_{222}], (d) butyl triethyl ammonium [N_{2224}], (e) N,N-diethyl-N-methyl-N(2-methoxyethyl) ammonium [$N_{221(1O2)}$].

Prior to characterisation and cell assembly, the ILs were heated under rapid stirring for several hours in an argon filled glovebox (H_2O<0.1ppm, O_2<0.1ppm). The moisture content of ILs dried using this technique was determined to be less than 7ppm using Karl Fischer titration (KF899 Coulometer, Metrohm). Viscosity was measured using a Bohlin Gemini (Malvern Instruments Ltd.) rheometer with 50mm diameter stainless steel conical plates (º1) using a gap size of 20µm for shear rates from 10 to 1000s^{-1}.

Electrochemical tests were carried out using a Solartron Analytical 1470E Multichannel Potentiostat/Galvanostat with 1455A Frequency Response Analysers. The electrochemical stability window of the ILs was determined using linear sweep voltammetry at 50mVs^{-1} in a three electrode setup using a glassy carbon working electrode (3mm dia.), Ag wire pseudo reference electrode and Pt wire counter electrode. Swagelok®-type symmetrical cells using non-porous electrodes were used to identify suitable operating potentials in a manner similar to that used in previous investigations. Linear sweep voltammetry was performed between 0 and 4.5V at 50mVs^{-1}, with operating potentials identified using a cut-off current of 30µAcm^{-2}.

2.3 EDLC assembly and characterisation

Two-electrode button cells (2016) were assembled using stainless steel spacers, paired electrodes, and glass fibre filter paper separator (Whatman, GF/F). The separator was soaked with the electrolyte under study and the cell components were then placed under vacuum in the glovebox antechamber for ca. 5 mins to encourage the impregnation of the electrolyte. Cells were then crimped closed inside the glovebox.

Electrochemical impedance spectroscopy (EIS) of symmetrical EDLCs was performed at a potential bias of 0.1V (vs OCP), using a 10mV perturbation over the frequency range 100kHz to 10mHz. Cells were also cycled Galvanostatically between 0V and the operating voltage at various rates between 0.1 and $10Ag^{-1}$ (where IR drop permitted) using an Arbin SCTS instrument. Specific capacitance values are based on the mass of active material and are expressed on a three-electrode basis. All measurements were performed in triplicate at 25ºC.

3 Results & Discussion

3.1 Viscosity of ionic liquids

Low viscosity is a desirable property in EDLC electrolytes as lower viscosities are associated with higher specific capacitances and lower cell resistances.[23] Viscosities determined for each of the ILs in this work are given in Table 1 along with literature values of conductivity and cation volumes calculated using the Molinspiration Property Calculation Service.[40] (For comparison, the volume of the $[Tf_2N]$ anion is 148Å^3).

The viscosity of $[S_{221}][Tf_2N]$ was determined to be 38.4mPa.s, which in broad agreement with that found in literature (lit.,[41] 36mPa.s). However, reports indicate that a significantly lower viscosity would be associated with $[S_{222}][Tf_2N]$ (lit.,[31, 42] 30-33mPa.s) which was not observed in this study; in this case, $[S_{222}][Tf_2N]$ exhibited a viscosity almost equal to that of $[S_{221}][Tf_2N]$. This may arise from differences in moisture content.

In contrast, the ammonium based ILs display relatively high viscosities resulting from their appreciably larger cation volumes. The viscosity of $[N_{2224}][Tf_2N]$ determined experimentally was 140.3mPa.s which also compares favourably with reported values (lit.,[43] 144.8mPa.s).

The ether group present in the $[N_{221(1O2)}]$ cation results in significantly lower viscosity, (as reported for other ILs that incorporate ether-bonds in alkyl side chains[33, 34]). Electron donation from the oxygen atom diminishes the charge of the cation resulting in weaker anion-cation interactions.[30] The viscosity observed for $[N_{221(1O2)}][Tf_2N]$ of 66.5mPa.s agrees with the majority of published values (lit.,[44, 45] 64mPa.s at 24ºC, 69mPa.s) however it is noted that this is substantially different from the value reported by Sato et al. (120mPa.s[30]). Again, this disparity may arise from differences in moisture content.

Table 1 Physical properties [a] of the ionic liquids used in this work

IL	η □□□□.□]	σ □□□ □□□□]	V_c [Å^3]	ESW [V]
$[S_{221}][Tf_2N]$	38.4	5.8[41]	116	3.8
$[S_{222}][Tf_2N]$	38.6	7.1[31]	133	2.8
$[N_{2224}][Tf_2N]$	140.3	1.3[43]	196	3.9
$[N_{221(1O2)}][Tf_2N]$	66.5	2.6[45]	171	4.7

[a] η represents viscosity (at 25ºC), σ conductivity (at 25ºC), V_c cation volume[40], ESW electrochemical stability window determined in a three electrode cell (cut-off current density 40μAcm^{-2})

From the properties given in Table 1 it can be anticipated that the sulfonium based ILs will be associated with increased values of specific capacitance, reduced resistances and better rate performance when compared with the ammonium ILs.

3.2 Electrochemical stability of ionic liquids

Table 1 also reports the ESW determined using linear sweep voltammetry in a three-electrode cell, with a cut-off current density of 40μAcm^{-2}. These conditions result in narrower ESWs when compared with the majority of those reported in the literature. For comparison, the ESW observed under these conditions for a 1 moll^{-1} solution of tetraethylammonium tetrafluoroborate ($TEABF_4$) in propylene carbonate was 4V.

ESWs are extremely sensitive to the conditions used to define them. The point at which the current density is deemed large enough to indicate significant electrolyte decomposition is fairly arbitrary. Several flaws in using this method to determine the operating voltage of devices have been raised, and alternative approaches explored.[46-49] As the ESW tends to be asymmetric with respect to the open circuit potential of symmetric EDLCs, the operating potential that can be used without appreciable electrolyte decomposition is often substantially lower than the full ESW.

Operating potentials for the symmetric cells used in this work were identified using symmetrical two electrode cells in a manner similar to that employed in previous investigations.[34, 38] (The operating potential determined under these conditions for a 1 moll^{-1} solution of $TEABF_4$ in propylene carbonate was 2.1V.) It is noted that higher operating potentials are achievable for these ILs, perhaps through the use of asymmetric electrode loadings to make fuller use of the ESW. The conservative values used herein minimise the possibility of surface area being rendered inactive by species generated by electrolyte decomposition.

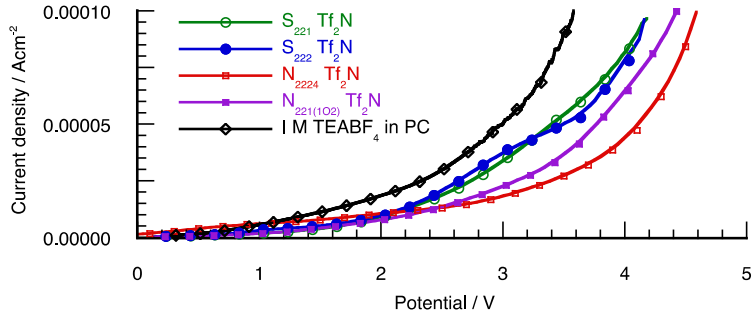

Fig. 2 Electrochemical stability of ionic liquids and a typical EDLC electrolyte determined in a symmetrical two-electrode cell at a sweep rate of $50mVs^{-1}$.

Figure 2 shows that there is little difference between the behaviour of the sulfonium based ILs. However it is worth noting that $[S_{221}][Tf_2N]$ is slightly more stable than $[S_{222}][Tf_2N]$ in both the three electrode and two electrode methods. This could suggest that the smaller cation volume of $[S_{221}][Tf_2N]$ influences the charge density of the ion resulting in slightly stronger ion-ion interactions.

A typical organic solvent-based electrolyte (1 $moll^{-1}$ $TEABF_4$ in propylene carbonate) is demonstrably less stable with increasing potential than the ILs as illustrated in Fig.2. It is also evident that the ammonium based Ls have greater electrochemical stability than the sulfonium ILs which can be mainly attributed to the difference in cation volumes.

The methoxyethyl group in the side chain of $[N_{221(1O2)}]$ reduces the positive charge density at the ammonium centre when compared with $[N_{2224}]$. For smaller cations, it has been reported that this results in a diminished ESW[33, 45] and this may be expected to occur in the case of $[N_{221(1O2)}][Tf_2N]$. However $[N_{221(1O2)}][Tf_2N]$ exhibits the widest ESW of the ILs studied using the three electrode method. It appears that the inclusion of the methoxyethyl group influences the degree of ionic coordination occurring and enhances the stability of the IL.[45] In contrast with the ESWs in Table 1, Figure 2 indicates that in a two-electrode configuration the ether bond reduces electrochemical stability, and the broader ESW seen in three electrode experiments does not result in an increased operating potential.

3.3 Characteristics of carbon materials

Pore characteristics of the activated carbon materials were investigated using nitrogen adsorption/desorption isotherms at -196ºC. Characteristics determined from the isotherms are given in Table 2. As the R/C ratio increases it can be seen that the specific surface area determined by both the BET and DFT methods increases There is no substantial change in the micropore volume, however it increases slightly with R/C ratio.

Table 2. Specific surface areas and pore characteristics calculated from nitrogen sorption isotherms at 77K.

□□	S_{BET}[a] [m^2g^{-1}]	S_{DFT}[b] [m^2g^{-1}]	V_{tot}[c] [cm^3g^{-1}]	V_{mic}[d] [cm^3g^{-1}]	V_{meso}[e] [cm^3g^{-1}]	d_{BJH}[f] [nm]	d_{DFT}[g] [nm]
200	**670**	**530**	**0.48**	**0.21**	**0.18**	**4.3**	**5.4**
250	720	580	0.53	0.22	0.21	5.1	6.3
300	**750**	**620**	**0.62**	**0.23**	**0.27**	**6.3**	**7.2**
350	790	630	0.67	0.24	0.32	7.5	8.1

[a] specific surface area calculated using the BET method [b]specific surface area determined using DFT model [c]total pore volume calculated at P/P_0>0.99 [d] micropore volume determined using the t-plot method [e] mesopore volume from DFT model [f] modal pore width estimated from BJH pore size distribution. [g]modal pore width estimated from DFT pore size distribution.

Mesopore volume increases markedly with increasing R/C ratio. This is illustrated in Figure 3, which shows the pore size distribution determined using the DFT model for each of the carbon materials in the small mesopore region. As the R/C ratio increases, the mode of the distribution shifts to larger pore sizes. Estimates of the modal pore width attributed to each material from the DFT model indicate that increasing the RC ratio by 50 in this region results in an increase in the average pore width of roughly 0.9nm. This trend was also observed when applying the BJH model to the desorption branch of the isotherms, as indicated by the values of d_{BJH} given in Table 2

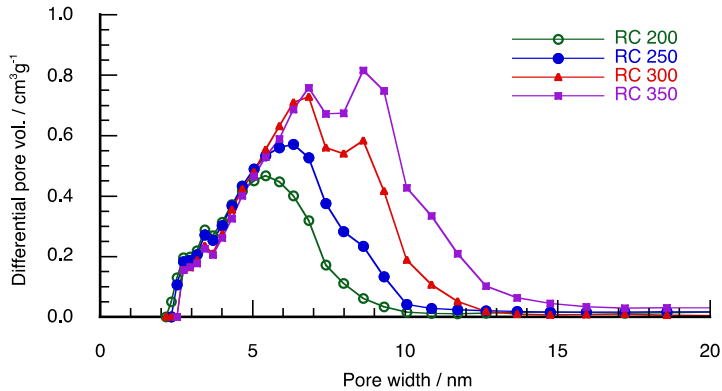

Figure 3. Mesopore size distribution of resorcinol formaldehyde derived activated carbon materials determined by the DFT model.

3.4 EDLC performance - sulfonium based ionic liquids

Firstly, considering the behaviour of cells assembled using sulfonium based ILs, where the cation volume is smaller than that of the anion, Figure 4(a) shows Nyquist plots produced using each of the carbon materials paired with $[S_{221}][Tf_2N]$. These spectra show that the cells do not behave as ideal capacitors, (i.e. vertical response at low frequencies) however at lower frequencies the response can be described as approaching ideal as the R/C ratio, and therefore pore width, increases. Increased pore widths are also associated with reduced specific capacitances as determined from the spectra at 10mHz. Cell characteristics obtained from the spectra are summarised in Table 3.

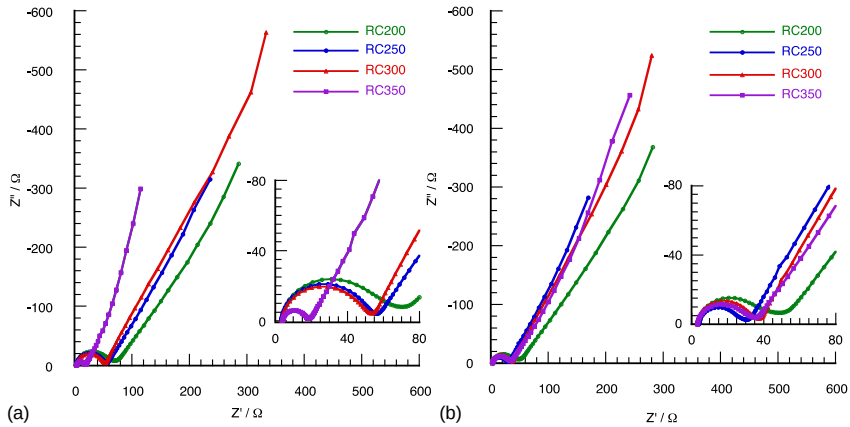

Fig.4 Nyquist plots obtained using electrochemical impedance spectroscopy for sulfonium based ionic liquids with controlled porosity carbons including magnified high-frequency regions (inset). (a) S_{221} Tf_2N and (b) S_{222} Tf_2N

Table 3. Cell characteristics for sulfonium based ionic liquids combined with controlled porosity carbon materials

IL	□□	□□□ □□□□□]	R_s [Ω]	R_i [Ω]	ESR [Ω]	$c_{0.2}$ □□□□□]	$c_{2.0}$ □□□□□]	R_{dc} [Ω]
[S_{221}][Tf_2N]	**200**	**27.4**	**3.4**	**55.3**	**41.1**	**39.1**	**17.1**	**39.6**
	250	26.8	3.2	48.3	37.9	43.0	23.0	37.7
	300	**18.1**	**3.3**	**46.3**	**36.9**	**32.2**	**17.4**	**32.2**
	350	24.3	4.2	13.6	17.0	38.7	27.5	10.0
[S_{222}][Tf_2N]	**200**	**22.8**	**3.9**	**35.9**	**31.9**	**35.4**	**16.4**	**26.1**
	250	26.1	4.2	22.7	24.2	40.5	24.5	19.8
	300	**18.0**	**3.0**	**30.9**	**29.0**	**28.8**	**16.5**	**25.5**
	350	19.2	3.4	28.2	26.1	29.5	17.5	21.1

[a] c_S represents the specific capacitance (determined using EIS at 10 mHz), R_s the series resistance, R_i ionic resistance, ESR equivalent series resistance (determined at 1 kHz), $c_{0.2}$ specific capacitance determined at a current density of $0.2Ag^{-1}$ (and $c_{2.0}$ at 2.0 Ag^{-1}) and R_{dc} represents the resistance determined using pulses of current at $2mAcm^{-2}$

The inset of Figure 4(a) shows a magnified section of the spectra at higher frequencies and their intersection with the real axis (R_s) varies little with the carbon used. It can also be seen that the increased pore width from RC200 to RC350 has an influence on the diameter of the semicircle that appears in the high frequency region. This diameter is influenced by ionic mobility and represents a measure of the ionic resistance (R_i). As the pore size increases, R_i and equivalent series of resistance (ESR) are seen to decrease. This trend is also seen in values of resistance (R_{dc}) determined from the iR drop using 10ms pulses at a current density of $2mA\ cm^{-2}$.

Increased resistances resulting from smaller pore sizes are also evident in Figure 5(a), where the variation of specific capacitance with rate is illustrated. At rates greater than ca. $5Ag^{-1}$ for RC200, the iR drop was greater than the operating voltage of the cell. The curves associated with each carbon material do not display any

obvious trend indicating that there are complicated relationships between the migration of ions, the packing of these ions at the electrode surface, and the pore characteristics of the electrode. Specific capacitances determined during Galvanostatic discharge at rates of $0.2Ag^{-1}$ ($c_{0.2}$) and $2.0Ag^{-1}$ ($c_{2.0}$) are given in Table 3. Unlike the specific capacitances determined using EIS, the values of $c_{0.2}$ and $c_{2.0}$ in Table 3 are noticeably higher when RC250 is coupled with $[S_{221}][Tf_2N]$ when compared with RC200 and RC300.

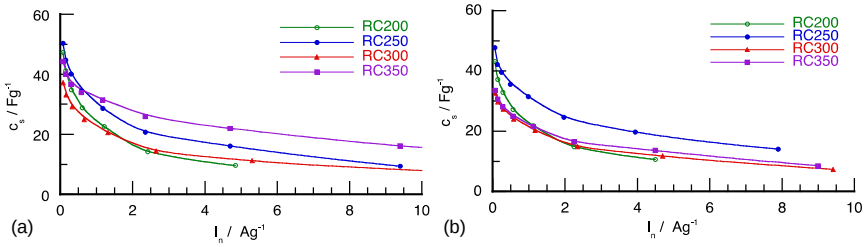

Fig. 5 Specific capacitance determined at different rates of constant current discharge between 0 and 2.5 V for cells using sulfonium based ILs. (a) $[S_{221}][Tf_2N]$ and (b) $[S_{222}][Tf_2N]$.

Considering the spectra in Figure 4(b), which shows the behaviour of cells produced with $[S_{222}][Tf_2N]$, it can again be seen that the cells do not display ideal capacitor behaviour and that there is no clear correlation between low frequency behaviour and variations in pore width.

From the detail in the inset of Figure 4(b), and the characteristics in Table 3, again it is seen that there is little variation in the values of R_s. However, unlike the cells using $[S_{221}][Tf_2N]$, there is no clear trend between the values of R_i, ESR or R_{dc} with the carbon material used. Specific capacitance is greatest when S_{222} Tf_2N is paired with RC250 and, moreover, R_i, ESR and R_{dc} are lowest for this combination. This supports the idea that the performance of ionic liquid based EDLCs can be improved by utilising carbon materials with carefully controlled pore characteristics.[37, 38] The highest values of R_i, ESR and R_{dc} were observed with the carbon displaying the narrowest pore size. This is due to the increased fraction of vacant pore volume in these electrodes, as a substantial fraction of pores are too narrow to accommodate electrolyte ions.

Figure 5(b) shows that the combination of RC250 with $[S_{221}][Tf_2N]$ unambiguously exhibits superior performance when compared with the other carbon materials.

Comparing the characteristics of cells using $[S_{221}][Tf_2N]$ with those using $[S_{222}][Tf_2N]$ there are marginally higher values of c_s and $c_{0.2}$ associated with $[S_{221}][Tf_2N]$ for each carbon material. This may result from a denser packing of ions under polarisation at the electrode surface, or the utilisation of a greater fraction of pores by the smaller $[S_{221}]$ cation. The absence of a methyl group in $[S_{221}][Tf_2N]$ may also reduce the distance between the charge centre of the adsorbed cation and the electrode surface, thereby displacing a greater amount of charge in the electrode.

Resistances (R_i, ESR and R_{dc}) exhibited by cells using $[S_{221}][Tf_2N]$ are larger than those using $[S_{222}][Tf_2N]$ when paired with RC200, 250 and 300. This could be

expected due to the lower conductivity of $[S_{221}][Tf_2N]$. Surprisingly when the sulfonium based ILs are paired with RC350, $[S_{221}][Tf_2N]$ displays substantially lower resistances despite exhibiting lower conductivity than $[S_{222}][Tf_2N]$. This is also evident when comparing the rate performance of the sulfonium based ILs paired with RC350 in Figure 5(a) and (b). It may be the case that by further increasing the pore width of the carbon a similar drastic reduction in resistances with $[S_{222}][Tf_2N]$ would be observed.

This behaviour may arise from the smaller cation volume of $[S_{221}][Tf_2N]$ influencing the properties of the electrode-electrolyte interphase as it can be anticipated that this region will display a conductivity mechanism different to that in than the bulk.

3.5 EDLC performance - ammonium based ionic liquids

Moving on to consider the behaviour of cells using ammonium based cations, where the volume of the cation is greater than that of the anion, spectra for cells generated using each of the carbons with $[N_{2224}][Tf_2N]$ are presented in Figure 6(a) and with $[N_{221(1O2)}][Tf_2N]$ in Figure 6(b). The most ideally capacitive behaviour is seen with RC300 for both ILs and furthermore, the highest values of specific capacitance and lower values of R_i and ESR are also observed with this carbon material.

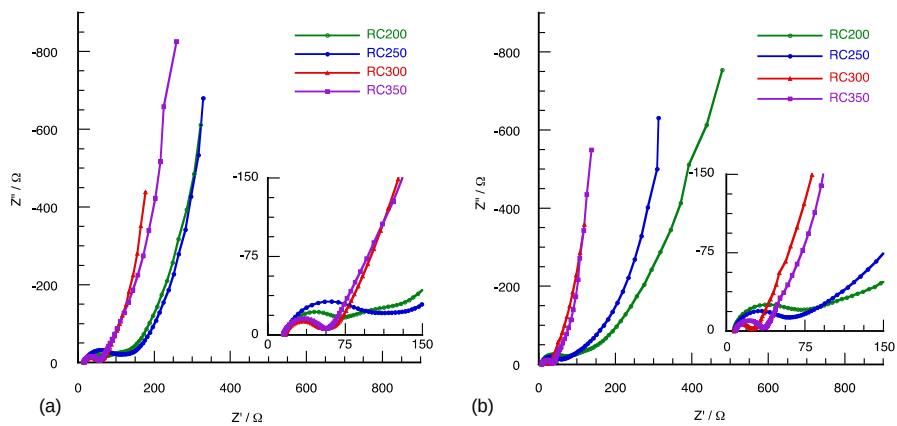

Fig. 6 Nyquist plots obtained using EIS for ammonium-based ILs with controlled porosity carbons including magnified high-frequency regions (inset). (a) $[N_{2224}][Tf_2N]$ and (b) $[N_{221(1O2)}][Tf_2N]$.

In Figure 6(a) RC200 and RC250 are seen to behave similarly when paired with $[N_{2224}][Tf_2N]$, however the increase in pore width to RC300 results in a marked decrease in R_i and increase in specific capacitance. This is also seen in the values of specific capacitance determined through Galvanostatic discharge. However it is noted that there is a substantial decrease in the value of c_s when RC350 is used that is not seen in the values of $c_{0.2}$ and $c_{2.0}$. This may be due to the high viscosity of $[N_{221(1O2)}][Tf_2N]$ hindering the perturbation signal at low frequencies. Nevertheless, Figure 7(a) shows that RC300 and RC350 behave almost identically with respect to rate and perform significantly better than RC200 and RC250.

Table 4. Cell characteristics[a] for sulfonium based ionic liquids combined with controlled porosity carbon materials

IL	□□	□□□ □□□□□□]	R_s [Ω]	R_i [Ω]	ESR [Ω]	$c_{0.2}$ □□□□□□]	$c_{2.0}$ □□□□□□]	R_{dc} [Ω]
$[N_{2224}][Tf_2N]$	**200**	**15.1**	**16.6**	**60.6**	**45.0**	**20.8**	**11.4**	**57.8**
	250	16.6	17.2	84.0	48.8	22.1	13.3	63.8
	300	**19.0**	**16.4**	**38.1**	**39.8**	**22.7**	**16.0**	**44.7**
	350	14.1	15.0	42.8	37.8	22.3	16.4	39.4
$[N_{221(1O2)}][Tf_2N]$	**200**	**16.3**	**7.4**	**61.3**	**42.1**	**23.6**	**12.0**	**46.5**
	250	17.4	8.0	48.7	37.9	27.5	19.3	38.7
	300	**22.7**	**7.4**	**16.0**	**21.6**	**28.4**	**23.2**	**19.4**
	350	17.2	9.0	26.7	27.8	23.8	18.4	22.3

[a] c_s represents the specific capacitance (determined using EIS at 10 mHz), R_s the series resistance, R_i ionic resistance, ESR equivalent series resistance (determined at 1 kHz), $c_{0.2}$ specific capacitance determined at a current density of $0.2 Ag^{-1}$ (and $c_{2.0}$ at $2.0 Ag^{-1}$) and R_{dc} represents the resistance determined using pulses of current at $2 mAcm^{-2}$

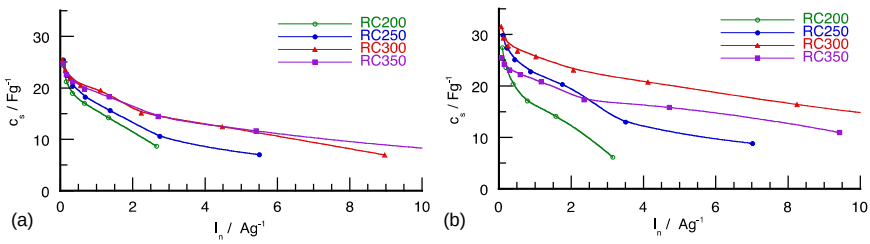

Fig. 7 Specific capacitance determined at different rates of constant current discharge between 0 and 3.0 V for cells using ammonium based ionic liquids and controlled porosity carbons. (a) $[N_{2224}][Tf_2N]$ and (b) $[N_{221(1O2)}][Tf_2N]$

$[N_{221(1O2)}][Tf_2N]$ could be expected to perform very differently to $[N_{2224}][Tf_2N]$ due to the lower cation size, lower viscosity and higher conductivity. An examination of Figure 6(b) shows that there are subtle differences between the behaviour of the ammonium based ILs. At first glance there are clear similarities between the spectra obtained for RC200 and RC250 paired with each of the ILs, and there are significantly smaller values of R_i for RC300, increasing slightly as the pore width widens to RC350.

On closer inspection there is a noticeable difference in the values of R_s; $[N_{221(1O2)}][Tf_2N]$ typically exhibits values of roughly 8Ω whereas $[N_{2224}][Tf_2N]$ consistently produces resistances around 16Ω. Also, despite the values of R_i associated with RC200 being similar, there is a noticeable difference in the magnitude of R_i for the other carbon materials. This is a result of the difference in conductivity of the IL which may be attributed to the presence of the ether bond in $[N_{221(1O2)}][Tf_2N]$. In the case of RC200 (which exhibits the narrowest pore size), a large fraction the resistance originates from the presence of empty pores and electrolyte conductivity has little influence on the value of R_i.

At high frequencies there is little difference between RC300 and RC350 in the case of $[N_{2224}][Tf_2N]$ however, as with the sulfonium based ILs, there is a minimum R_i that coincides with a peak specific capacitance when RC300 is paired with

$[N_{221(1O2)}][Tf_2N]$.

From Figure 7(a) and (b) it can be seen that $[N_{221(1O2)}][Tf_2N]$ displays better performance than $[N_{2224}][Tf_2N]$ when paired with each of the carbons and that it is clear that the best performance is a combination of RC300 with $[N_{221(1O2)}][Tf_2N]$. Interestingly, Figure 7(b) shows distinct kinks in the performance curves for the carbons possessing the narrower pore sizes, (RC200 and 250) which are not present in the curves obtained using the other ILs. This may indicate the existence of a greater degree of ionic coordination resulting from the ether bond.

4 Conclusions

Ionic liquids were studied in relation to their performance as electrolytes in EDLCs with carbon electrodes possessing different pore characteristics. ILs consisting of sulfonium cations paired with the bis(trifluoromethanesulfonyl) imide anion generally produced greater specific capacitances and lower resistances than the ammonium based ILs studied. This behaviour can be attributed to their smaller cation size, which strongly influences physical properties such as viscosity and ionic mobility. However it was seen that the ammonium based cations led to increased electrochemical stability, indicating that higher operating potentials, are achievable with these electrolytes.

As the R/C ratio of the carbon precursor increased, mesopore volume and the average pore width increased, allowing for the comparison of EDLC performance with electrodes possessing different slightly different pore characteristics. Despite displaying similar physical properties, the sulfonium based ILs performed remarkably differently with respect to pore width. The marginally smaller cation ($[S_{221}]$) performed better with the carbon exhibiting the largest pore width whereas peak performance for $[S_{222}][Tf_2N]$ was associated with a narrower pore size. A substantial reduction in resistance was observed at the larger pore width for $[S_{221}][Tf_2N]$ which is likely to be responsible for the improved performance.

Considerable differences between the performance of the ammonium based ILs were found and are related to their physical properties. In this case it is not only the smaller cation volume but also the inclusion of a methoxyethyl group in place of an ethyl side chain that affect physical properties and results in substantially improved electrochemical performance. This may be related to electron donation from the oxygen atom influencing the charge density of the cation and facilitating cation-cation interactions.

This study suggests that by altering the structure of the ions in the IL and by careful control of the pore characteristics of the electrode, the performance of EDLCs can be improved substantially. The development of more conductive and electrochemically stable ILs, coupled with tailored electrode materials, will enhance the energy density that can be attained by EDLCs and broaden the range of applications where they are employed.

[a] Dept. of Chem. & Bio. Eng., University of Sheffield, Sheffield, S1 3JD, UK Fax: (+)44 114 222 7501; Tel: (+)44 114 222 8257; E-mail: a.rennie@sheffield.ac.uk

References

1. B. E. Conway, Electrochemical Supercapacitors - Scientific Fundamentals and Technological Applications, Plenum, New York, 1999.

2. A. Burke, J. Power Sources, 2000, **91** 37–50.
3. A. G. Pandolfo and A. F. Hollenkamp, J. Power Sources, 2006, **157**, 11-27.
4. R. Kötz and M. Carlen, Electrochim. Acta, 2000, **45**, 2483–2498.
5. P. J. Hall, M. Mirzaeian, S. I. Fletcher, F. B. Sillars, A. J. R. Rennie, G. O. Shitta-Bey, G. Wilson, A. Cruden and R. Carter, Energy Environ. Sci., 2010, **3**, 1238.
6. J. R. Miller and A. F. Burke, Electrochem. Soc. Interface, 2008.
7. P. G. Simon, Y, Nat. Mater., 2008, **7**, 845-854.
8. E. Frackowiak and F. Béguin, Carbon, 2001, **39**, 937–950.
9. J. R. Miller and P. Simon, Science, 2008, **321**, 651-652.
10. P. Simon and Y. Gogotsi, Acc. Chem. Res., 2013, **46**, 094–1103.
11. M. Winter and R. J. Brodd, Chem. Rev., 2004, **104**, 4245-4269.
12. E. Frackowiak, Q. Abbas and F. Béguin, J. Energy Chem., 2013, **22**, 226-240.
13. J. M. Blanes, R. Gutiérrez, A. Garrigós, J. L. Lizán and J. M. Cuadrado, IEEE Trans. Power Electronics, 2013, **28**, 5940-5948.
14. R. Carter, A. Cruden and P. J. Hall, IEEE Trans. Veh. Technol., 2012, **61**, 1526-1533.
15. N. Omar, J. Van Mierlo, B. Verbrugge and P. Van den Bossche, Electrochim. Acta, 2010, **55**, 7524-7531.
16. R. A. Huggins, Solid State Ionics, 1996, **86-88**, 41-48.
17. A. Brandt, S. Pohlmann, A. Varzi, A. Balducci and S. Passerini, MRS Bull., 2013, **38**, 554-559.
18. M. Armand, F. Endres, D. R. MacFarlane, H. Ohno and B. Scrosati, Nat. Mater., 2009, **8**, 621-629.
19. M. C. Buzzeo, R. G. Evans and R. G. Compton, Chem.Phys.Chem., 2004, **5**, 1106-1120.
20. M. Galiński, A. Lewandowski and I. Stępniak, Electrochim. Acta, 2006, **51**, 5567-5580.
21. T. Welton, Chem. Rev., 1999, **99**, 2071−2083.
22. R. Mysyk, V. Ruiz, E. Raymundo-Piñero, R. Santamaria and F. Béguin, Fuel Cells, 2010, **10**, 834-839.
23. F. B. Sillars, S. I. Fletcher, M. Mirzaeian and P. J. Hall, Phys. Chem. Chem. Phys., 2012, **14**, 6094-6100.
24. D. R. MacFarlane, J. Sun, J. Golding, P. Meakin and M. Forsyth, Electrochim. Acta, 2000, **45**, 1271-1278.
25. R.-S. Kühnel and A. Balducci, J. Power Sources, 2014, **249**, 163-171.
26. C. Arbizzani, M. Biso, D. Cericola, M. Lazzari, F. Soavi and M. Mastragostino, J. Power Sources, 2008, **185**, 1575-1579.
27. A. Balducci, R. Dugas, P. L. Taberna, P. Simon, D. Plée, M. Mastragostino and S. Passerini, J. Power Sources, 2007, **165**, 922-927.
28. M. Lazzari, F. Soavi and M. Mastragostino, Fuel Cells, 2010, **10**, 840-847.
29. A. B. N. McEwen, H. L.; LeCompte, K.; Goldman, J. L., J. Electrochem. Soc., 1999, **146**, 1687−1695.
30. T. Sato, G. Masuda and K. Takagi, Electrochim. Acta, 2004, **49**, 3603-3611.
31. H. Matsumoto, T. Matsuda and Y. Miyazaki, Chem. Lett., 2000, 1430-1431.
32. D. Wei and T. W. Ng, Electrochem. Commun., 2009, **11**, 1996-1999.
33. M. J. Monteiro, F. C. Camilo, M. C. C. Ribeiro and R. M. Torresi, J. Phys. Chem. B, 2010, **114**, 12488−12494.
34. A. J. R. Rennie, N. Sanchez-Ramirez, R. M. Torresi and P. J. Hall, J. Phys. Chem. Lett., 2013, **4**, 2970-2974.
35. C. O. Ania, J. Pernak, F. Stefaniak, E. Raymundo-Piñero and F. Béguin, Carbon, 2006, **44**, 3126-3130.
36. C. Arbizzani, S. Beninati, M. Lazzari, F. Soavi and M. Mastragostino, J. Power Sources, 2007, **174**, 648-652.
37. S. Pohlmann, B. Lobato, T. A. Centeno and A. Balducci, Phys. Chem. Chem. Phys., 2013, **15**, 17287-17294.
38. F. B. Sillars, S. I. Fletcher, M. Mirzaeian and P. J. Hall, Energy Environ. Sci., 2011, **4**, 695-706.
39. A. J. R. Rennie and P. J. Hall, Phys. Chem. Chem. Phys., 2013, **15**, 16774-16778.
40. Molinspiration Cheminformatics, http://www.molinspiration.com.
41. S. Fang, L. Yang, C. Wei, C. Peng, K. Tachibana and K. Kamijima, Electrochem. Commun., 2007, **9**, 2696-2702.
42. H. Matsumoto, H. Sakaebe and K. Tatsumi, J. Power Sources, 2005, **146**, 45-50.
43. Z. Wang, Y. Cai, T. Dong, S. Chen and X. Lu, Ionics, 2013, **19**, 887–894.

44. T. Kondoh, A. Asano, J. Yang, K. Norizawa, K. Takahashi, M. Taguchi, R. Nagaishi, R. Katoh and Y. Yoshida, Radiat. Phys. Chem., 2009, **78**, 1157-1160.
45. Z. B. Zhou, H. Matsumoto and K. Tatsumi, Chem. - Eur. J., 2005, **11**, 752-766.
46. D. Weingarth, A. Foelske-Schmitz and R. Kötz, J. Power Sources, 2013, **225**, 84-88.
47. D. Weingarth, H. Noh, A. Foelske-Schmitz, A. Wokaun and R. Kotz, Electrochim. Acta, 2013, **103**, 119-124.
48. K. Xu, M. S. Ding and T. R. Jow, Electrochim. Acta, 2001, **46**, 1823-1827.
49. K. Xu, S. P. Ding and T. R. Jow, J. Electrochem. Soc., 1999, **146**, 4172-4178.

Acknowledgements

The authors are indebted to the EPSRC for funding (EP/K021192/1).